2018 IEEE Intelligent Vehicles Symposium (IV)
Changshu, Suzhou, China, June 26-30, 2018

A Fusion of a Monocular Camera and Vehicle-to-Vehicle Communication for Vehicle Tracking: An Experimental Study

Mustafa Tekeli[1] and Çağdaş Yaman[1] and Tankut Acarman[1], *Member, IEEE,* and Murat Akın[1]

Abstract— In this paper we present the procedure of fusing a monocular camera based vehicle tracking and IEEE 802.11p Vehicle-to-Vehicle communication enabled position, velocity and time sharing. Toward a monocular camera-based detection and tracking, Haar-like features of a vehicle are trained, median flow tracking algorithm is applied, pixel based relative distance and relative speed is estimated. In order to improve reliability and availability of tracking system, IEEE 802.11p radio modem is added. Then, we implement Particle Filter algorithm in order to fuse the information provided by these two sensors subject to different characteristics. We evaluate the tracking system by the real road data collected on highway. Sensor fusion results along different road scenarios are presented. We present the state-of-the-art low cost sensor fusion, our application setup and elaborate some experimental results.

I. Introduction

Sensing and tracking the surrounding objects in the road traffic is an important requirement toward decision making about safe maneuvering tasks in intelligent vehicles (IVs). But the stand-alone performance of sensor can be poor due to its sensitivity and not being immune to various environment conditions. Fusion of sensors with different characteristics can improve reliability and availability of the information provided by the sensing and tracking system. In this paper, our particular focus is on the preliminary results of demonstration study and deployment of vehicle tracking system by fusing a mono camera-based detection and tracking, and shared position, velocity and time (PVT) provided by a Global Navigation Satellite System (GNSS) receiver via IEEE 802.11 vehicle-to-vehicle communication (V2V) radio modem in Vehicular Ad-hoc Network (VANET).

Some sensors such as cameras, microwave sensors and LIDAR have limited performance and accuracy. For instance, detection with standard vision sensors would be inaccurate at longer distances due to reduced resolution and immunity to ambient conditions such bad weather and sudden changes in lighting. Also, LIDARs are still expensive and they require high computational power while computing boards in vehicles tend to be small and cost effective. Microwave radars are also used in today's automotive technology, however they suffer from reflections caused by concrete objects on the road.

In this paper, we demonstrate the experimental results of a particle filter algorithm using a mono camera and IEEE 802.11p modem with a GNSS receiver. The paper is organized as follows: related work is presented in Section II. Detection and tracking for each stand-alone sensor is briefly presented in Section III. Then, particle filter is revisited for relative positioning. Road experiments and usability of the presented fusion approach is presented in Section IV. Finally, some conclusions are given.

[1]Authors are with Computer Engineering Department, Galatasaray University, 34349, Istanbul, Turkey

(corresponding author: Tankut Acarman, e-mail: tacarman@gsu.edu.tr).

II. Related Work

Object detection plays a crucial role for active safety. Vehicle detection by fusing radar and vision sensor is used to automatically activate car's emergency braking system in [1]. Although radar's detection performance in the radial direction is high, it is poor in the azimuth direction, which causes false detection of a preceding vehicle in the same lane. And false detection causes false activation of automatic emergency braking. Fusion with a camera-based vehicle recognition method and detection of shape and motion improves the reliability of vehicle detection system. In [2], lane departure warning system is presented. This system uses Doppler effect to detect the frequency shift in reflected waves and vision-based camera to recognize the patterns on the road such as lane-marking, front vehicle, road sign and other obstacles. In [3], a fusion of radar and vision for vehicle detection is presented. The guard rail detection and a method to handle the overlapping areas is described. The radar data is used to locate the areas of interest on the images to perform the detection task. Vehicles detected in different image regions are combined together and a series of filters is applied to remove false detections. This system correctly and precisely detects the closely located vehicles.

An intelligent, camera-assisted system capable of interpreting its surroundings on real-time basis is presented in [4]. A combination of color, edge and motion information is used to detect vehicles, road boundaries and lane markings on the road. Stereo vision based obstacle and lane detection is studied in [5]. Both generic obstacles and lanes are detected at 10 Hz while using a specific hardware for image processing, and perspective effect from stereo images was removed. They used left vision sensor to detect lane marking while remapped stereo images were used to detect free space.

An extended SIFT feature description method is applied to achieve robust vehicle tracking in [6] but more efforts are needed to improve real-time performance. In [7], a pre-crash vehicle detection system is developed and different feature extraction methods and classifiers are evaluated to assure real-time operability.

III. Detection And Tracking

A. Camera-based Vehicle Detection

Haar feature-based cascade classifier, whose features and efficiency has been improved in [8] and originally proposed in [9], is developed for detection purposes. Haar classifier is trained with 550 positive and 500 negative sample images with a resolution of 100x40 pixels. Sample image dataset is

provided by UIUC Image Database for Car Detection in [10]. For feature extraction, Canny edge detection in [11] is applied and pixel sum difference between black areas and white areas is calculated by using integral image in (1),

$$ii(x,y) = \sum_{x' \le x, y' \le y} i(x',y') \quad (1)$$

the extracted features are listed in Table I.

TABLE I: USED HAAR FEATURES IN OPENCV LIBRARY FROM [8]

Edge features								
Line features	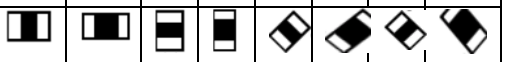							
Center-surround features	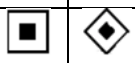							

Motivated by [12], pixel based inter-vehicle distance estimation is implemented to compute the relative distance between the leading and ego vehicle. The proposed algorithm obligates the vision sensor to be mounted at a tilt angle so that the projection of the lower bound of image corresponds with the distance between the front of the car and camera sensor. However, hood of the car is in the field of view (FOV) of the sensor, which disturbs edge and feature detection. Therefore, the tilt angle is adjusted to make visible the road scene at lower part of the frame. Finally, for relative distance estimation, the following mounting angle is applied:

$$d_2 = \tan(\theta_c \pm \beta) \times H \quad (2)$$

$$D = d_2 - d_1 \quad (3)$$

where H denotes the camera height in mm, θ_c is the angle between the local vertical and lateral camera axis denoted by Z_c and $-Y_c$, d_1 is the distance between camera, D is the distance between the leading and ego vehicle, respectively. FOV of the camera is given in terms of focal length of the lens, sensor width and height as follows:

$$\propto = 2 \times \tan^{-1}\left(\frac{H/2}{f}\right) \quad (4)$$

$$\beta = 2 \times \tan^{-1}\left(\frac{W/2}{f}\right) \quad (5)$$

where W is the sensor width in mm, f is the focal length in mm, $\propto$ is the vertical FOV and β is the horizontal FOV. This information is provided in manufacturer's datasheet.

B. Tracking and Relative Speed Estimation

Median flow tracker measures the differences caused by the occlusions between video frames to detect failure [13]. Given the pair of images and a bounding box, which is a region-of-interest (ROI) in the case of vehicle tracking, it generates a set of points inside a ROI and applies Lucas-Kanade tracker to compute sparse motion flow between frames. Each point is assigned with an error and according to the quality of prediction, points subject to error higher than 50% are considered as outliers and they are removed. The remaining points are used to estimate the consecutive displacement of the ROI.

Toward validation and road demonstration, each of the tracked ROIs is either given an incremental unique ID or assigned ID is maintained during tracking. Estimation of the relative speed of the vehicle based on the distance travelled is calculated as follows:

$$V_r = 3600 \times \frac{\pm\Delta_d}{1000/H} \quad (6)$$

C. Transmission of PVT via V2V communication

Wireless communication between vehicles enables information exchange without requiring any fixed infrastructure or base station. The location and velocity of vehicles is constantly changing and the RF communication range is fairly short distance. Therefore, the set of vehicles that can directly communicate, constantly changes over a short period of time. This dictates that the physical layer and the network must be capable of operating in an ad hoc, decentralized manner, although coordination and synchronization through GNSS time signals is feasible.

In order to comply with the European Profile Standard ITS-5G defined in ETSI EN 302 571, IEEE 802.11p physical and MAC layers are implemented [14]. Cooperative Awareness Messages (CAM) broadcast with a value of 19 dBm on the 10 Mhz channel at 5.9 GHz with a data rate of 3 Mbit/s. CAM message rate is 1 Hz with an antenna transmission range about 300 meters.

The main goal of this study is to demonstrate fusion of two sensors and improve availability of measurement. Neighbor vehicle's position and speed is measured from two different sensors, namely camera and PVT measured by a GNSS receiver and transmitted by a IEEE 802.11p radio modem. The camera provides the pixel based position information in 2D that is later used for estimating the local coordinates X and Y in meters as well as the distance and relative speed in kmph. However, IEEE 802.11p radio modem transmits the geographic coordinate information of the GNSS receiver, which is latitude, longitude and altitude of the surrounding vehicle, and GNSS PVT of the ego vehicle is also measured for relative position, relative velocity calculation. To align global and local measurements, we convert latitude, longitude and altitude measurement to the global earth-centered, earth-fixed (ECEF) coordinates in meters. Then, the differences in ECEF coordinates between surrounding vehicle and ego vehicle are converted to east, north, up (ENU) local coordinates. Since we convert the difference of ECEF coordinates, we obtain the difference in ENU coordinates that provides east, north and up difference in meters between the surrounding vehicle and ego vehicle. But however, we need the information about X, Y and distance towards the detected surrounding vehicle subject to ego vehicle's measured heading. Using the rotation matrix with heading information and local ENU position vector, we compute the relative distance in 2D in the local coordinate system.

IV. SENSOR FUSION

A moving vehicle is considered for localization. Motion model linear in the state dynamics and non-linear in the measurements is given by,

$$\mathrm{x}_t = A\mathrm{x}_{t-1} + Bu_{t-1} + f_t \quad (7)$$

$$z_t = h(x_{t-1}) + e_{t-1} \quad (8)$$

where the state-space of the relative positioning filter consists of the position in the longitudinal and lateral direction, and altitude (x, y, γ) in the ECEF ("Earth-Centered, Earth-Fixed") coordinate system [15]. For vehicle detection, altitude is assumed to be known and state to be estimated is represented as a two-dimensional vector $x_t = [x, y]^T$ at time index t. Measured input is the odometer, which is angular wheel speed of the ego vehicle $u_t = w_{wheel}$ provided by the on-board diagnostic (OBD) of the vehicle, and faults are denoted by f_t. Measurement vector is constituted by the physical sensors that are a GNSS receiver and a camera providing relative position, relative velocity estimation, denoted by n_t and s_t, respectively. Hence, $z_t = [n_t \;\; s_t]^T$ is the measurement suite, and e_t denotes the measurement error vector.

Particle filter is a numerical approximation to the Bayes Filters. The sampling importance resampling (SIR) algorithm is one of the most widely used sequential Monte Carlo methods, which allow the system state estimation to be computed on-line while the state changes as it is the case for tracking algorithms. A SIR filter usually manages a fixed number of possible system state hypotheses x_t^i, where superscript i denotes the *i-th* individual particle. These individual particles approximately generate the distribution of the system state, $p(X_t)$. The SIR algorithm is computed at each discrete time step.

Posterior probability $p(x_t \mid Z_t)$ is approximated by a weighted sample set of particle filters. A basic framework with particle filters for localization problems in different application areas introduced by [16]. This approach converts computationally expensive integral calculation into the simple summation procedures. The stages of the particle filter implementation can be stated as follows:

- Initialize the individual particles $x_0^i \sim p_{x0}$ for i = 1,…,N
- Measurement update, update particle weights by use of likelihood
$$w_t^i = w_{t-1}^i \, p(z_t \mid x_t^i), \text{ for } i = 1,\ldots,N$$
- Normalize weights such that total of weights is equal to zero, $\hat{x}_t \approx \sum_{i=1}^{N} w_t^i x_t^i$ is an approximation.
- Resampling: If number of efficient samples is below a certain value, resampling is required. The value for efficient samples, denoted by N_{eff}, is dependent on N. If the ESS is smaller than this threshold, only small portion of particles are contributing to the estimation. In this case, particles with small weight are deleted. Weights are normalized at the stage of mean calculation,
$$N_{eff} = \frac{1}{\sum_i (w_i^t)^2} \quad (9)$$
- Transition: According to the motion model, particles are updated.

After initialization of particles, the measurement is updated for state transition of the initialized particles. The angular wheel speed is measured by the odometer, and then velocity of the ego vehicle is calculated. Based on the updated velocity information, denoted by v_{t-1} at time index $t-1$, a state transition is calculated as arbitrary movement on 2D plane. State transition model is given by:

$$x_t = x_{t-1} + 2T_s v_{t-1} cos(\alpha) \quad (10)$$
$$y_t = y_{t-1} + 2T_s v_{t-1} sin(\alpha) \quad (11)$$

where T_s is the sampling interval and α denotes a uniformly distributed random angle in the interval of $[0, 360^0]$. The ego vehicle's velocity is multiplied by a factor of two to prevent the prediction bias, which may be caused by high error values of relative distance computation based on follower-leader vehicle's GNSS measurements.

For each particle, initial weight is calculated based on the possibility derived by the measurements of GNSS position and camera-based relative position. Probability is calculated under the assumption that the deviations of the GNSS and camera-based measurements are normally distributed and standard deviation is changed with respect to the confidence values. Weights are normalized then location information is calculated by use of linear weights. All the information is stored in the array of estimation.

The relation between the weight of the *i-th* particle and the probabilities at the time instance t is as follows:

$$w_t^i \; \alpha \; P(n_t, s_t \mid x_t^i) = P(n_t \mid x_t^i).P(s_t \mid x_t^i) \quad (12)$$

For $i = 1,\ldots,N$, where N is the number of particles, and t is the time index. Weight update of the particles based on GNSS measurement is given as follows:

$$[w_t^i]_{x_{GNSS}} = a e^{-1/2([x_t]_{GNSS} - [x_t^i])^2 / \sigma_x^2}$$
$$[w_t^i]_{y_{GNSS}} = b e^{-1/2([y_t]_{GNSS} - [y_t^i])^2 / \sigma_y^2} \quad (13)$$

where $a = 1/(\sigma_x \sqrt{2\pi})$, $b = 1/(\sigma_y \sqrt{2\pi})$, σ_x^2 and σ_y^2 denotes the variance of the GNSS position measurement error in both of the horizontal and lateral direction, respectively. These values are calculated as a function of measurement reliability such as Horizontal and Vertical Dilution of Precision (HDOP, VDOP) $\sigma_x^2 = 10HDOP$ and $\sigma_y^2 = 10VDOP$.

Weight update of the particles based on relative positioning measured by a camera is given as follows:

$$[w_t^i]_{x_{Camera}} = c_{Camera} e^{-1/2([x_t]_{Camera} - [x_t^i])^2 / \sigma_{Camera}^2}$$
$$[w_t^i]_{y_{Camera}} = c_{Camera} e^{-1/2([y_t]_{Camera} - [y_t^i])^2 / \sigma_{Camera}^2} \quad (14)$$

where $c_{Camera} = 1/(\sigma_{V2V} \sqrt{2\pi})$, and σ_{Camera}^2 denotes the variance of relative positioning based on camera detection. A normal distribution in a variate is denoted by each particle

coordinate with mean $([x_t]_{GNSS}, [y_t]_{GNSS})$ related to GNSS measurement and $([x_t]_{Camera}, [y_t]_{Camera})$ ToA measurement and variance (σ_x^2, σ_y^2) , σ_{Camera}^2 , respectively [17].

V. Experimental Study

For experimental purposes, three vehicles are equipped with a IEEE 802.11p radio modem and a GNSS receiver connected in an automotive grade mini-PC for PVT sharing purposes. The ego vehicle has also an Ethernet camera sensor and an IMU to measure the ego vehicle's transient motion and camera-based tracking algorithm. The camera has 1080 pixel resolution with an Ethernet interface. FOV is calculated as 31° in the horizontal and 23° in the vertical axis. The height of camera is measured 117 cm while tilt angle is measured -1°.

During the road experiment, sensor data was stored in a laptop PC on the ego vehicle. Stored data is the data transmitted in VANET via IEEE 802.11p radio modems, ego vehicle's PVT data, and acceleration and angular velocity data provided by a GNSS receiver and inertial motion unit (IMU), respectively. This information is time-stamped with the ego vehicle's GNSS receiver UTC time and extended with the tracking results gathered from live frames provided by the camera sensor. The camera sensor was set at 20 fps and each CAM message transmitted by the two neighbor cars in the antenna transmission range is associated to a frame number that corresponds to the current frame retrieved from the camera.

At the first stage, the stand-alone performance of camera-based detection and tracking is elaborated. Once the vehicle is detected, a representative ROI is created. This individual ROI is either red or blue colored depending on its detection score. If the score is below a certain threshold, the detected window is shown in red, otherwise it is colored in blue. Furthermore, to enhance the stability of ROI tracking and to avoid occlusions with the surrounding objects in highly dynamic traffic scenes, the applied tracker does not directly use the detection ROI, but it generates and tracks a smaller portion of that image, which is shown in blue. For instance, a road scene is given in Figure 1.

The classifier is also evaluated with vision benchmark of KITTI video set from [18]. The sample scene from this data is plotted in Figure 2. A comparison is made by using both data and performance of camera based classifier is evaluated in Table II. To enhance tracking performance, particle filter is applied. To visualize results of each camera-based tracking and detection by PVT sharing via V2V communication, a birds-eye-view visualization interface is used. Ego vehicle is located at the center given by (0,0) and other surrounding vehicles are relatively located. This visualization interface having a range of 90 meters in the longitudinal direction is divided into the grid with a size of 3 meters. The stand-alone detection and particle filter tracking results are plotted in Figure 3 through Figure 5. In Figure 6, the white colored light commercial vehicle (lcv) with an ID 67 and the brown vehicle ID 66 equipped with a IEEE 802.11p modem is detected by both camera and their shared PVT data in VANET. As a result, on the left side of interface in Figure 3, the first and third line presents relative position and velocity update computed by shared PVT of each vehicle with respect to ego vehicle's PVT provided by its own GNSS receiver. The second and fourth line presents the result of tracking and vehicle classification algorithm based on camera sensor. The particle filter algorithm fuses these two sensor measurements. The number of particles is chosen 200. Under the assumption that the road is flat, and the full range of ambient conditions such as lighting, shadowing and reflection does not degrade detection performance, and open sky condition holds in the highway, the measurement variance of vision-based sensing and GNSS receiver measurement error variance is taken 3 meters and 5 meters based on the previous experiment statistical results, respectively. The particle filter result for each neighbor car is plotted by colored balls at the vicinity of measurements plotted by colored squares in Figure 3, is closer to camera-based detection measurement since its variance is smaller than GNSS-based relative distance calculation. In the following driving sequence plotted by Figure 4 and in Figure 7, the ego vehicle was making a left change, is increasing its speed and approaching to other two V2V equipped vehicles on their oncoming left lane. In Figure 4, white lcv with an ID 68 is not camera detected but it is in the right adjacent lane of the ego vehicle and in its radio transmission range; it is correctly located and tracked via its shared PVT as the result of particle filter algorithm.

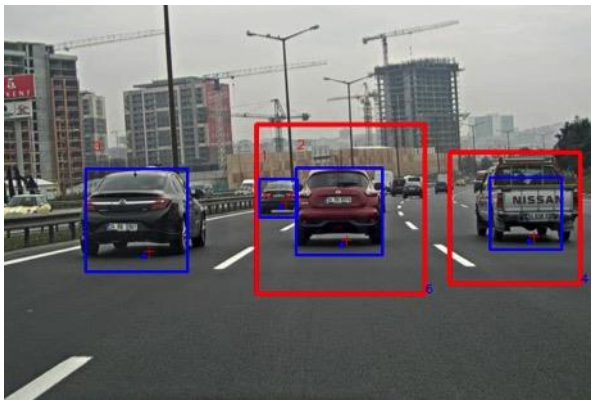

Figure 1: Detection and tracking of vehicles

Figure 2: Detection result with a sample in KITTI dataset

Table II: Comparison of TPR (or recall), PPV (or precision) for KITTI vision benchmarking set and road data collected in İstanbul.

Dataset	TP	FP	FN	TPR	PPV
KITTI	26	9	6	81.25%	74.28%
Our Road Data	30	2	8	78.94%	93.75%

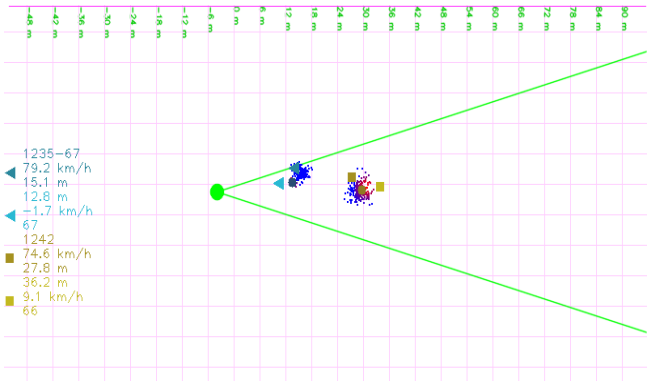

Figure 3:Visualization of tracking and estimation for the scene in Figure 6.

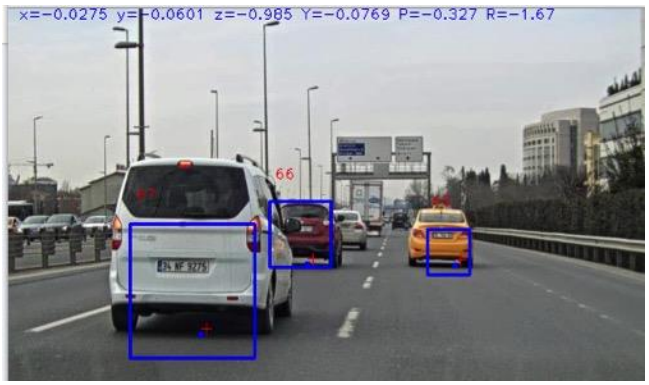

Figure 6: Tracking scene

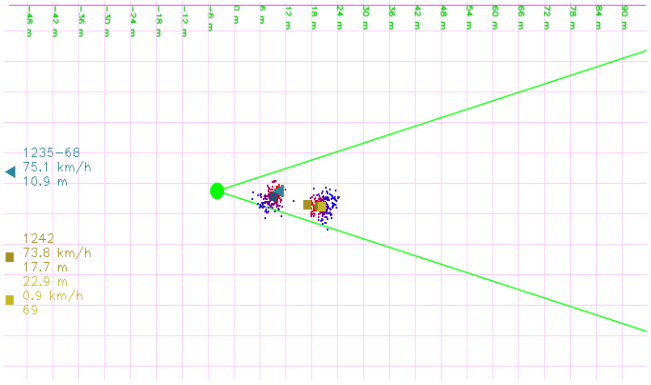

Figure 4: Visualization of tracking and estimation for the scene in Figure 7.

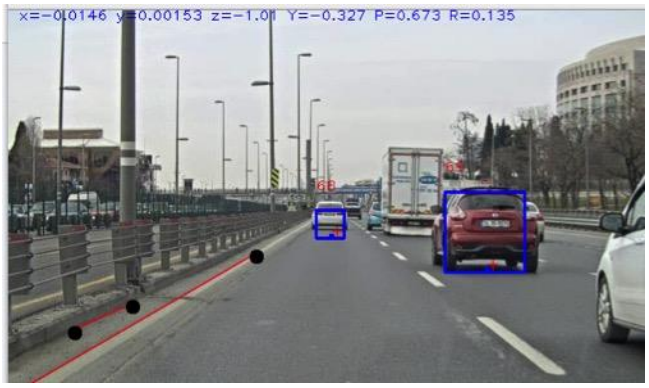

Figure 7: Tracking scene

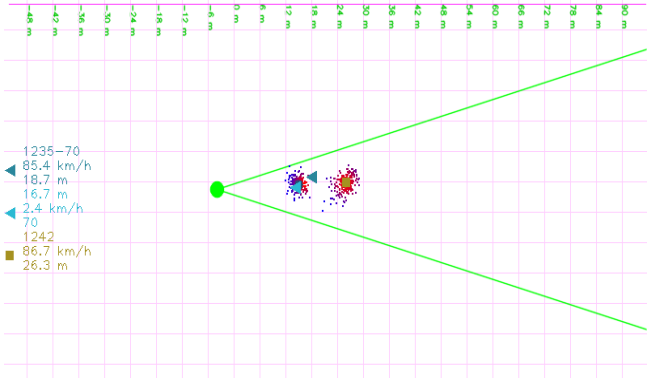

Figure 5: Visualization of tracking and estimation for the scene in Figure 8.

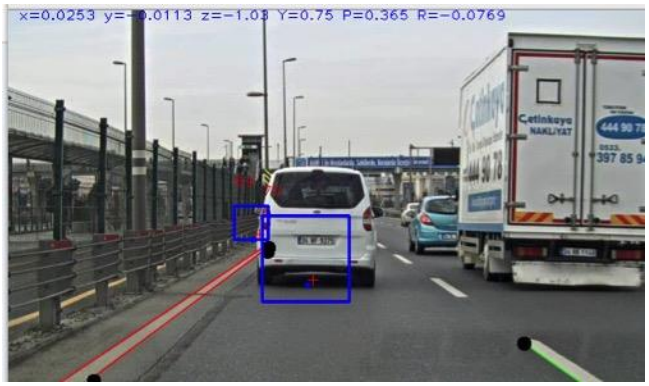

Figure 8: Tracking scene

And, brown vehicle with an ID 69 is both tracked and detected via camera and its PVT sharing. In Figure 8, two vehicles to be detected are on the left lane. The white lcv with an ID 70 is in the middle between ego and the first vehicle, i.e., the brown vehicle with an ID 69 and occlusion is occured for the camera but both vehicles are in the radio transmission range and CAM messages are successfully received by the ego vehicle. Particle filter is succesful at tracking the occluded vehicle while predicting the relative distance and velocity in the third line of the visualization interface. The first 6500 camera frames aligned with shared PVT of two vehicles in VANET are plotted in Figure 9 and Figure 10. Figure 9 presents the relative distance estimated by camera-based detection (red dot line) and relative distance calculated as the result of PVT sharing in VANET (blue dashed line) for the vehicle denoted by 1235 in Figure 3 thru Figure 5. Particle filter assures reliability and availability of measurements provided by sensor with different characteristics. In Figure 9, the vehicle denoted by 1235 disseminated 6154 CAM messages with 1 Hz frequency, which were successfully received by the ego vehicle but the tracked vehicle was not sensed by the camera for the total of 3425 instances versus the total of 6154 isntances. Figure 10 presents the detection and particle filter prediction results for the vehicle denoted by 1242. And 6136 CAM messages were successfully transmitted to the ego vehicle but for the total of 4162 instances, this surrounding vehicle 1242 was not detected by the camera. Particularly, due to low GNSS measurement frequency, i.e., 1 second, significant deviations and jumps are plotted

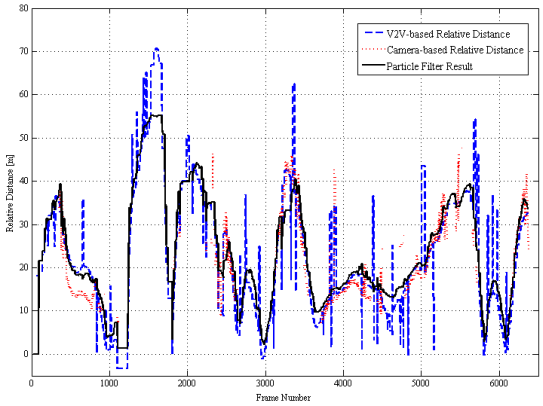

Figure 9: The frame results of relative distance predicted by camera-based tracking and V2V transmitted GNSS PVT data for white lcv car denoted by 1235. Particle filter assures availability of relative positioning.

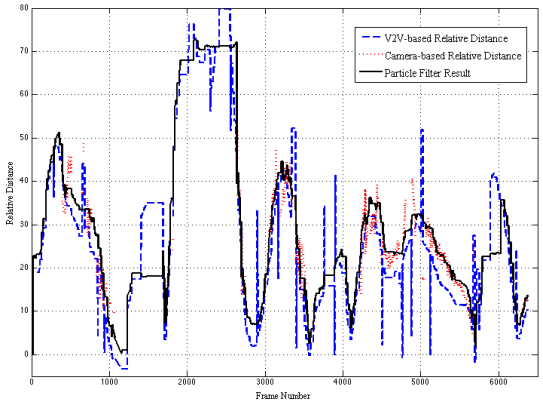

Figure 10: The frame results of relative distance predicted by camera-based tracking and V2V transmitted GNSS PVT data for brown car denoted by 1242.

between two consecutive position measurements. But particle filter enables smooth multiple vehicle tracking.

VI. Conclusion

In this paper, we demonstrate the experimental results of a particle filter algorithm using a mono camera and a IEEE 802.11p modem with a GNSS receiver. The vehicle classifier is trained by a fairly large dataset and a new tracker system is adapted to estimate pixel based relative distance and relative speed. Real road data from both highway and urban areas in Istanbul was collected. Stand-alone detection performance of camera-based system is evaluated by comparing KITTI vision benchmark and our own dataset. Then, detection system is augmented by V2V communication and sensor fusion is applied. Mono camera and 360^0 coverage provided by V2V communication improves availability of detection and tracking of neighbor vehicles.

Acknowledgement

The authors gratefully acknowledge the support of Galatasaray University, scientific research support program under grant # 17.401.001.

References

[1] Kim H, and Song B., Vehicle Recognition Based on Radar and Vision Sensor Fusion for Automatic Emergency Braking, 13th International Conference on Control, Automation and Systems, Kimdaejung Convention Center, Gwangju, Korea, pp.1342-1346, 2013.

[2] Huo C, Yu Y, and Sun T., Lane Departure Warning System based on Dynamic Vanishing Point Adjustment, The 1st IEEE Global Conference on Consumer Electronics, Makuhari Messe, Tokyo, Japan, pp.25-28, 2012.

[3] Alessandretti G, Broggi A, and Cerri P., Vehicle and Guard Rail Detection Using Radar and Vision Data Fusion, IEEE Transactions on Intelligent Transportation Systems: Vol.8, No.1: 95-105, 2007.

[4] Betke M, Haritaoglu E, and Davis L. S., Real-time multiple vehicle detection and tracking from a moving vehicle, Machine Vision and Applications, New York: Springer-Verlag, pp.69-83, 2000.

[5] Bertozzi M, and Broggi A., GOLD: A Parallel Real-Time Stereo Vision System for Generic Obstacle and Lane Detection, IEEE Transactions on Image Processing: vol.7, no.1:, pp.62-81, 1998.

[6] Yıldız R, and Acarman T., Image Feature Based Video Object Description and Tracking, IEEE International Conference on Vehicular Electronics and Safety, İstanbul, TURKEY, pp.405-411, 2012.

[7] Sun Z, Bebis G, and Miller R., Monocular Precrash Vehicle Detection: Features and Classifiers, IEEE Transactions on Image Processing: vol.15, no.7:, pp.2019-2034, 2006.

[8] Lienhart R, Kuranow A, and Pisarevsky V, Empirical Analysis of Detection Cascades of Boosted Classifiers for Rapid Object Detection, Pattern Recognition: 25th DAGM Symposium, Magdeburg, Germany, pp.297-304, 2003.

[9] Viola P, and Jones M.,Rapid Object Detection using a Boosted Cascade of Simple Features, IEEE Conference on Computer Vision and Pattern Recognition, Kauai, Hawaii, USA, pp.I-511-518, 2001.

[10] Agarwal S, Awan A. Roth D. UIUC Image Database for Car Detection. URL: https://cogcomp.cs.illinois.edu/Data/Car/

[11] Canny J, A Computational Approach to Edge Detection, IEEE Trans. on Pattern Analysis and Machine Intelligence: 8(6), pp.679-698, 1986.

[12] Rezaei M, Terauchi M, and Klette R., Robust Vehicle Detection and Distance Estimation Under Challenging Lighting Conditions, IEEE Transactions on Intelligent Transportation Systems: vol.16, no.5:2015, pp.2723-2743, 2015.

[13] Kalal Z, Mikolajczyk and K, Matas J., Forward-backward error: Automatic detection of tracking failures, IEEE 20th International Conference on Pattern Recognition, Istanbul, Turkey, pp.2756-2759, 2010.

[14] ETSI EN 302 637-2 V1.3.2. Intelligent Transport Systems (ITS); Vehicular Communications;"Basic Set of Applications; Part 2: Specifications of Cooperative Awareness Basic Service".

[15] Ü. Özgüner, T.Acarman, and K. Redmill, "Autonomous Ground Vehicles", Artech House Publisher, Norwood, MA, 2012.

[16] F. Gustafsson, F. Gunnarson, N. Bergman, U. Forssell, J. Jansson, R. Karlsson, and P. Nordlund, "Particle Filters for Positioning, Navigation and Tracking", IEEE Transactions on Signal Processing, vol. 50, No. 2, pp. 425 – 437, February 2002.

[17] Peker, AU, Acarman, T. "VANET-Assisted Cooperative Vehicle Mutual Positioning: Feasibility Study", IEICE Transactions on Fundamentals of Electronics, Communications and Computer Sciences, vol. E100.A, no.2, pp.448-456, 2017.

[18] Geiger A, Lenz P, Stiller C, and Urtasun R. "Vision meets robotics: The KITTI dataset", The International Journal of Robotics Research: vol.32, no.11, pp.1231-1237, 2013.